Applied Catalysis B: Environmental 98 (2010) 65–71

Contents lists available at ScienceDirect

Applied Catalysis B: Environmental

journal homepage: www.elsevier.com/locate/apcatb

Electroreduction of carbon dioxide at a lead electrode in propylene carbonate: A spectroscopic study

B. Eneau-Innocent[a,b], D. Pasquier[b], F. Ropital[b], J.-M. Léger[a], K.B. Kokoh[a,*]

[a] LACCO UMR-CNRS 6503, «Equipe Electrocatalyse», Department of Chemistry, Université de Poitiers, 40, avenue du Recteur Pineau, 86022 Poitiers cedex, France
[b] IFP, 1 et 4, avenue de Bois Préau–92852 Rueil-Malmaison cedex, France

ARTICLE INFO

Article history:
Received 31 January 2010
Received in revised form 26 April 2010
Accepted 1 May 2010
Available online 9 May 2010

Keywords:
Pb electrode
CO_2 reduction
In situ IR reflectance spectroscopy
Propylene carbonate
Oxalate

ABSTRACT

The electrochemical reduction of carbon dioxide at a lead electrode was studied in propylene carbonate (PrC) containing tetraethylammonium perchlorate (TEAP) as electrolyte. Different electrochemical techniques such as cyclic voltammetry and chronoamperometry were used to evaluate the catalytic activity of this material towards CO_2 electrodimerization. The electroreduction process was also investigated by *in situ* infrared reflectance spectroscopy in order to determine adsorbed intermediates and reaction products. The peak of reduction observed in cyclic voltammetry starting at −2.05 V *vs.* Ag/AgCl has been clearly ascribed to the carbon dioxide reduction by SPAIRS technique. Infrared reflectance spectroscopy also confirmed the absence of CO at the lead cathode during chronoamperometric measurements and that oxalate has been formed concurrently to the CO_2 consumption. Combining the analytic and spectroscopic results, a reaction mechanism was proposed for the reduction of carbon dioxide to oxalate ions on a lead cathode in a nonaqueous aprotic medium.

1. Introduction

Carbon dioxide (CO_2) is considered as the main contributor to the greenhouse effect due to energy-related activities, industrial processes and waste combustion. Although the development of sequestration technologies which involve its capture and secure storage is receiving considerable attention, its conversion to environmentally neutral species has been the focus of a number of recent studies [1–9]. Different ways to reduce CO_2 have been investigated, such as chemical, thermochemical, photochemical, biochemical and electrochemical procedures. This abundant literature shows the electrochemical reduction of CO_2 to be a promising process for the synthesis of added value products [8,10–13], with two main parameters controlling the selectivity:

(1) *The nature of the electrocatalyst*: In aqueous solution most materials used as planar electrodes led to the formation of either carbon monoxide or formic acid [10,14–17]. The metals of the sp group (Pb, Tl, In, Zn, Sn, Hg, Cd) tend to favour the formation of formic acid, while other metals such as (Pt, Ni, Ag, Au) show a greater activity towards the CO_2 reduction with a strong adsorption potential leading to the formation of carbon monoxide in aqueous solution and even more to small amounts of hydrocarbons such as methane, ethane and ethylene, which can be used as gaseous fuel [18–21]. However in water the more active the metal is, the more preponderant is the hydrogen evolving coming from the water reduction. Otherwise, we recently showed in a filter-press cell that the synthesis of formate on Pb strongly depends on the pH value of the catholyte (in the range pH 8.6) where the acid–base equilibrium indicates that HCO_3^- is the predominant species in aqueous solution [22]. The main reaction could be written:

$$HCO_3^- + H_2O + 2e^- \rightarrow HCOO^- + 2HO^- \quad (1)$$

which is in competition with the water reduction:

$$2H_2O + 2e^- \rightarrow H_2 + 2HO^- \quad (2)$$

(2) *The nature of the solvent*: Many researchers have actively studied the electrochemical reduction of CO_2 using various metals in organic solvents [8,9,23,24]. Conversely to water, the merits of nonaqueous solvents include a higher solubility of CO_2 and a larger cathodic potential window, so avoiding the hydrogen evolution reaction (HER) as a competing process. It was also reported that in aprotic solvents, such as dimethyl sulfoxide (DMSO), N,N-dimethyl formamide (DMF), propylene carbonate (PrC) and acetonitrile (ACN), metals such as Sn, Pb, In, Hg would lead to form oxalic acid as the main product, while on Pt, Pd, In, Zn, Sn, Au cathodes, carbon monoxide and carbonate are the major products [2,23,24]. Formate and other glyoxylate and glycolate ions are also encountered but result in the pro-

* Corresponding author. Tel.: +33 5 49 45 4120; fax: +33 5 49 45 3580.
E-mail address: boniface.kokoh@univ-poitiers.fr (K.B. Kokoh).

0926-3373/$ – see front matter
doi:10.1016/j.apcatb.2010.05.003

tonation of carbon dioxide or oxalate ions, respectively [9,25], traducing the presence of water or other protic solvents in the aprotic medium. In nonaqueous aprotic media, two main competitive pathways have been described in the literature [10], the first one, resulting in the dimerization of $CO_2^{\bullet-}$ to form the oxalate anion [10,23] and the second reaction route including the adsorption of carbon dioxide at the electrode and leading to the dismutation of carbon dioxide and thus to the formation CO and CO_3^{2-} [9,10,23].

Otherwise, some papers reported intermediates species studied by spectroscopic techniques during electroreduction of CO_2 [9,26–28]. Bockris and co-workers reported an *in situ* IR spectroscopic study of electrochemical reduction of CO_2 at a Pt electrode in a nonaqueous electrolyte. They observed spectral bands assigned to CO_2^- [29,30]. Beden et al. revealed by infrared spectroscopy that the well known "reduced CO_2", formed on Pt electrode surfaces immersed in CO_2-saturated electrolyte (0.5 M H_2SO_4), is adsorbed CO [31–34]. Hori et al. confirmed the presence of adsorbed CO on a Cu electrode by Fourier Transform Infrared (FTIR) spectroscopy [8,35–37]. Ortiz et al. investigated by *in situ* FTIR spectroscopy the electrochemical reduction of CO_2 on different electrodes in methanol containing 0.1 M sodium perchlorate. It was concluded from the FTIR spectra obtained that there was no reduction of CO_2 on any of the metals studied (Sn, Cu, In Au, Ni, Ru, Pt), and that the only reaction product detected by FTIR spectroscopy, *was* carbonate, formed by reaction of CO_2 with hydroxyl anions produced in the electroreduction of residual water [9].

The present work is mainly focused on the electrochemical reduction of CO_2 to oxalate at a lead electrode in a nonaqueous and aprotic electrolyte (0.2 M tetraethylammonium perchlorate–propylene carbonate). According to the literature [23,24], the experiments carried out in propylene carbonate allow the orientation of CO_2 reduction towards its dimerization, while the presence of H_2O molecules leads to the hydrogenation reaction with the production of formate. Propylene Carbonate was chosen for its ability to solvate CO_2 in high quantity (0.14 mol L^{-1} at 25 °C, 1 bar) [38], its large electrochemical window and its relatively low toxicity compared to other aprotic solvents. To investigate this reaction, we combine cyclic voltammetry (CV) and *in situ* IR reflectance spectroscopy measurements which provide new insights into the comprehension of the reaction mechanism of the CO_2 reduction process.

2. Experimental

2.1. Voltammetry experiments

Voltammetry experiments were carried out in a one-compartment conventional three-electrode Pyrex cell (V = 15 cm^3). The working electrode was a lead wire (99.9% from Alfa Aesar®) with a geometric surface area of 0.42 cm^2. The current densities were normalized with the geometric surface area. A vitreous carbon plate and Ag/AgCl immersed in the solution served as counter and reference electrodes, respectively. Voltammetry measurements were performed with an Autolab PGSTAT 302 Electrochemical Interface at controlled temperature using a cryostat bath.

Concerning the cyclic voltammetry measurements performed at different temperatures (Arrhenius equation), CO_2 saturation of the electrolyte was started at the highest temperature (25 °C) before subsequent cooling to insure a constant CO_2 concentration in the electrolyte within the whole temperature range explored.

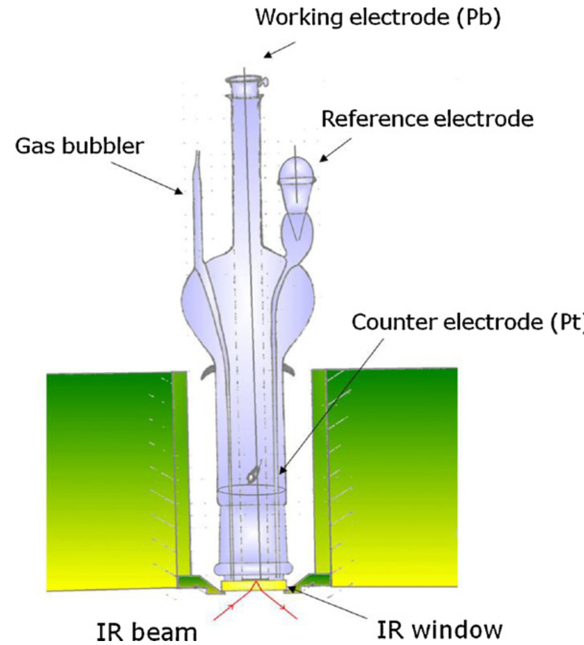

Fig. 1. Infrared spectroelectrochemical cell.

2.2. Fourier transform IR spectroscopy

A special three-electrode spectroelectrochemical cell (Fig. 1) was designed with CaF_2 IR transparent windows allowing the beam to pass through a thin electrolyte layer and to be reflected at the incidence angle of 65°. The Pb working electrode (lead Plate 99.9% from Alfa Aesar®) was a disc of 8 mm diameter. This electrode was mechanically polished to a mirror-finish with alumina (up to 0.3 μm). The counter electrode was a plate of vitreous carbon and the reference electrode was Ag/AgCl directly immersed in the solution.

IR reflectance spectra in the region 1000–3000 cm^{-1} were collected by a Bruker IFS 66 v/S Fourier transform infrared spectrometer. As previously described, this apparatus was equipped with a spectral reflectance device allowing the observation of reflectance spectra at the electrode–electrolyte interface with the IR light beam passing entirely through a chamber under vacuum [39]. It was also equipped with a helical globar light source and a liquid nitrogen-cooled mercury–cadmium-telluride (MCT) narrow-band detector (Infrared Associates). Data acquisition and processing were performed using OPUS 5.5 software. Different methods were used to obtain FTIR spectra: Single Potential Alteration Infrared Reflectance Spectroscopy (SPAIRS) and Chronoamperometry/FTIRS. In the SPAIRS technique [40,41], the electrode reflectivity R_i is recorded at different potentials E_i at 50 mV intervals during the first voltammetric sweep at 1 mV s^{-1}. Each IR spectrum is the Fourier transform of the average of 128 co-added interferograms. Spectra were calculated as $-\Delta A = \Delta R/R = (R_{E2} - R_{E1})/R_{E1}$, where the "reference" spectrum, R_{E1}, was that recorded at −3.0 V *vs.* Ag/AgCl. In the second technique, spectra were recorded at different times (t = 0, 20, 40, 60, 120, 180, 240 and 300 s) with the cathodic potential set at −2.5 V *vs.* Ag/AgCl. Spectra were calculated as $-\Delta A = \Delta R/R = (R_t - R_{t(\mathrm{Ref})})/R_{t(\mathrm{Ref})}$, where the "reference" spectrum, $R_{t(\mathrm{Ref})}$, was that recorded at t = 0 or 300 s.

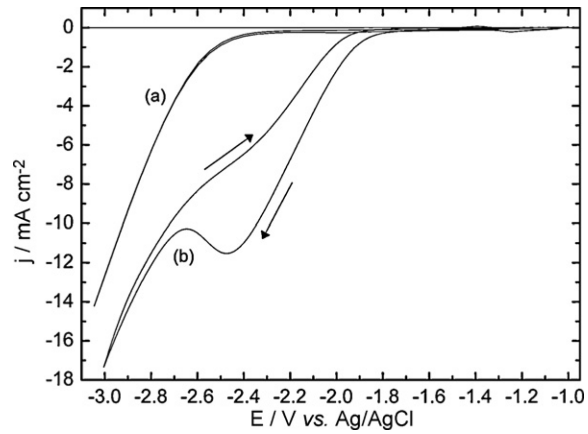

Fig. 2. Voltammograms of a Pb electrode in 0.2 M TEAP–PrC recorded at 50 mV s^{-1} and 25 °C in the absence (a) and the presence of a CO_2-saturated solution (b).

3. Results and discussion

3.1. Voltammetry study of CO_2 in propylene carbonate at lead electrode

Cyclic voltammograms on the lead electrode in 0.2 M TEAP–PrC were recorded with a potential sweep rate at 50 mV s^{-1} and at 25 °C in the absence (Fig. 2a) and the presence (Fig. 2b) of CO_2-saturated solution.

As can be observed in Fig. 2a, no reduction wave is obtained in the absence of CO_2. The voltammogram of Pb in Fig. 1b was recorded after bubbling CO_2 during 15 min. During the negative going scan the cathodic current starts increasing at −2.05 V *vs.* Ag/AgCl and reaches a maximum of −11.3 mA cm^{-2} at −2.5 V *vs.* Ag/AgCl.

In order to identify the rate determining step of CO_2 reduction, CV experiments were performed (Fig. 3) at various potential sweep rates. As described by the Randles–Sevcik equation, for a mass transfer process, the peak current should be proportional to the square root of the sweep rate [42]:

$$j_P = 0.4463nFC_{CO_2}\sqrt{\frac{nFD}{RT}} \times \sqrt{\nu} \tag{3}$$

where n is the number of electrons, ν is the scan rate (V s^{-1}), F is Faraday's constant, R is the universal gas constant, T is the absolute temperature, C_{CO_2} the concentration of CO_2 and D is the diffusion coefficient of the analyte. As expected for a mass transfer controlled process, the plot of peak current *vs.* the square root of scan rate yields a straight line (Fig. 4) [42–44].

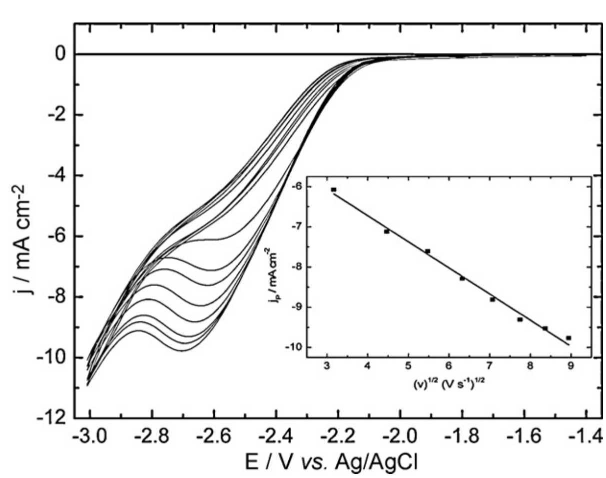

Fig. 3. Voltammograms of a Pb electrode in 0.2 M TEAP–PrC in the presence of CO_2-saturated, recorded at various potential sweep rates from 10 to 100 mV s^{-1}; in the inset the Randles–Sevcik plot.

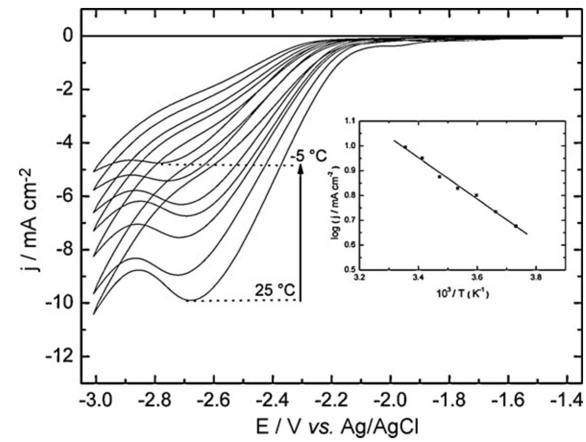

Fig. 4. Voltammograms of a Pb electrode in 0.2 M TEAP–PrC in the presence of CO_2-saturated, recorded from 25 to −5 °C; in the inset the plot of log(j) *vs.* T^{-1}.

The effect of temperature was also investigated from 25 to −5 °C as pointed out above, and the cyclic voltammograms at 50 mV s^{-1} are reported in Fig. 4 (inset). The increase of temperature increases the current density, while the peak potential shifts. The corresponding activation energy (ΔH^*), is estimated by the use of the Arrhenius equation:

$$\left[\frac{\partial \log j_P}{\partial(1/T)}\right]_{E_P,C} = \frac{-\Delta H*}{2.3R} \tag{4}$$

where j_P is the peak current density value at the peak potential (E_P = −2.6 V *vs.* Ag/AgCl); R is the universal gas constant (8.314 J mol^{-1} K^{-1}).

The value of ΔH^* (18 kJ mol^{-1} *i.e.* lower than 50 kJ mol^{-1}), the CO_2 reduction reaction involved during the peak is controlled by an irreversible diffusion process [43].

3.2. Spectroscopy study

To obtain further information about intermediates and reaction products formed during the electrochemical conversion of CO_2 at a Pb electrode, *in situ* IR reflectance spectroscopy measurements were performed in a 0.2 M TEAP-PrC solution. Prior to these measurements, characterization of the electrolytic solution (TEAP-PrC) was carried out in order to differentiate the bands due to the solvent and those of CO_2 and its reduction products.

Although the recording of the reference spectra of formic acid (Fig. 5c), oxalic acid (Fig. 5d), the electrolyte (TEAP-PrC) (Fig. 5a) and CO_2 (Fig. 5b) were performed, respectively, in this order, it can be observed, in Fig. 5a, c and d, that a weak band due to CO_2 appears at 2341 cm^{-1}. This did not disturb the subsequent attribution during the electrochemical experiment since the SPAIR spectra were normalized as pointed out in the experimental section. In order to propose a plausible reaction mechanism, the adsorbed intermediates and the electroreduction products near the lead electrode surface were determined both by SPAIRS and SPAIRS/chronoamperometry.

Reference spectra of 0.2 M TEAP-PrC, oxalic and formic acids, and CO_2 in 0.2 M TEAP-PrC were calculated with a reference spectrum taken recorded at −2.8 V *vs.* Ag/AgCl (Fig. 5). The spectra are normalized as follows:

$$\frac{\Delta R}{R} = \frac{R_{sol} - R_{el}}{R_{el}} \tag{5}$$

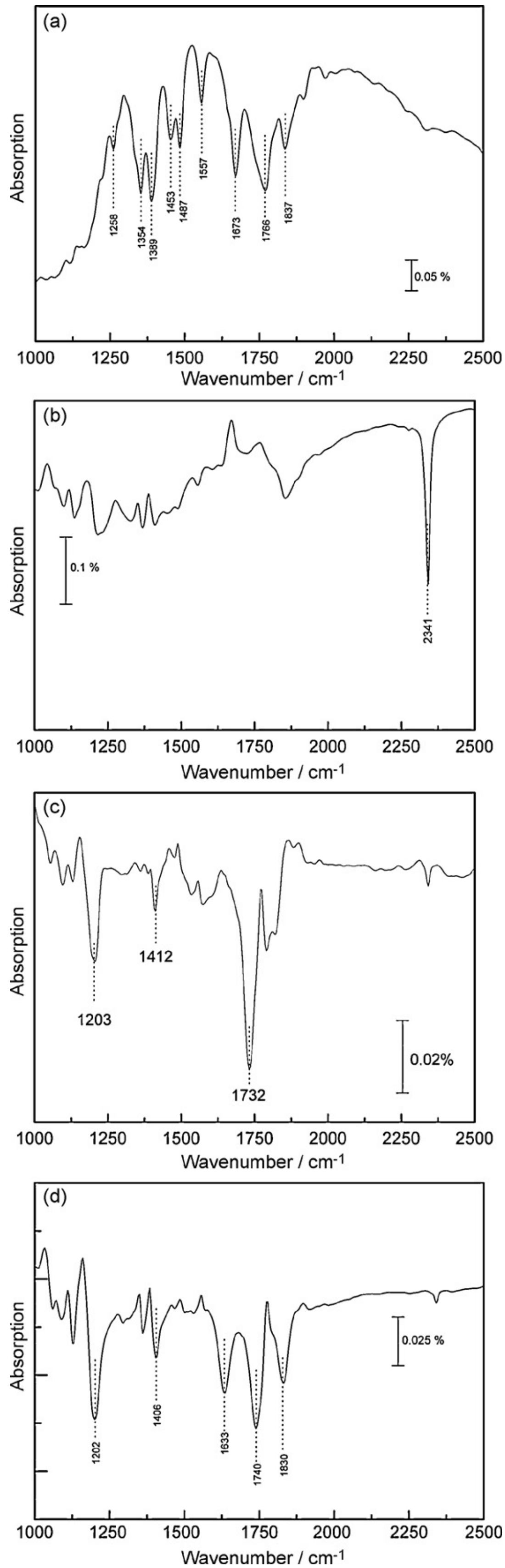

Fig. 5. Reference spectra of 0.2 M TEAP–PrC recorded at −2.8 V *vs*. Ag/AgCl (a), CO_2 (b), formate (c) and oxalate (d) recorded in 0.2 M TEAP–PrC.

Table 1
Characteristic infrared bands (wavenumbers in cm^{-1}) of reference compounds in 0.2 M TEAP-PrC.

Compounds				
TEAP-PrC	CO_2 in TEAP-PrC	Oxalic acid in TEAP-PrC	Formic acid in TEAP-PrC	Assignments [9,45–47]
		1200	1203	$\nu_{C–O}$
1353				$HC–CH_{bend}$
1386				CH_{rock}
		1407	1412	δ_{OCO}
1453				C–C–H (CH_3)
1482				CH_{bend} (CH_3)
1557				CH_{def} (CH_3)
		1631		$\nu_{C–C}$
		1741	1732	$\nu_{C=O}$
1769				/
1839				$C=O_{str}$
	2341			CO_2

where R_{sol} is the reflectivity of the electrode surface in a 0.2 M TEAP-PrC solution containing a studied molecule (CO_2, oxalate or formate); R_{el} represents the reflectivity of the Pb surface in the only electrolytic solution. This calculation minimizes the bands of the electrolyte by retaining only those of the investigated compounds.

Assignments were made according to the literature [9,45–47]; the main bands observed in Fig. 5 are listed in Table 1.

As can be seen, oxalate and formate have common bands at 1200 cm^{-1} (oxalate)/1203 cm^{-1} (formate); 1407 cm^{-1} (oxalate)/1412 cm^{-1} (formate); 1741 cm^{-1} (oxalate)/1732 cm^{-1} (formate); two of these bands are close to those of the electrolytic solution (TEAP-PrC) at 1453 and 1769 cm^{-1}. Oxalate has a band at 1631 cm^{-1} which enables it to be distinguished from formate. It is attributable to the vibration of the C–C bond in oxalate, the only bond that is not common with formate.

3.3. SPAIR spectroscopy

The SPAIRS technique which allows detection of intermediates and reaction products, consists in recording the reflectivities at 50 mV intervals during the first voltammetric scan at a sweep rate of 1 mV s^{-1}. This allows to correlate the appearance and disappearance of some characteristic vibration bands with potential. SPAIR spectra recorded after bubbling CO_2 for 15 min in a 0.2 M TEAP-PrC solution are depicted in two parts with respect to the amplitude (Fig. 6a and b). Spectra were calculated with the "reference" spectrum, R_{E1}, which is recorded at −3.0 V *vs*. Ag/AgCl, *i.e.* where all CO_2 species could be considered consumed. Therefore, the normalization related to this reference spectrum allows the reduction of CO_2 to be followed (Fig. 7).

The characteristic bands of the electrolyte (0.2 M TEAP–PrC) at 1260 and 1669 cm^{-1} were observed. At −1.4 V *vs*. Ag/AgCl (Fig. 6a), the band centred at 2341 cm^{-1} confirms the presence of CO_2 in the solution. The intensity of this band decreases with the cathodic potential. At −2.4 V *vs*. Ag/AgCl (Fig. 6b), the band due to CO_2 is not visible, this species is entirely consumed. From these spectra the intensity of the band due to CO_2 can be measured and is presented according to the cathodic potential (Fig. 7). Conversely to the results reported in the literature [8], no traces of CO (band at *ca*. 2037 cm^{-1}) [9] were visible in different spectra recorded. From this absence, it can be inferred a selective reduction of CO_2 at a Pb electrode in propylene carbonate medium.

Fig. 7 shows that after −1.8 V *vs*. Ag/AgCl, the band intensity of CO_2 decreases, traducing the beginning of the CO_2 reduction at this potential. From −2.4 V *vs*. Ag/AgCl, CO_2 is totally reduced at the

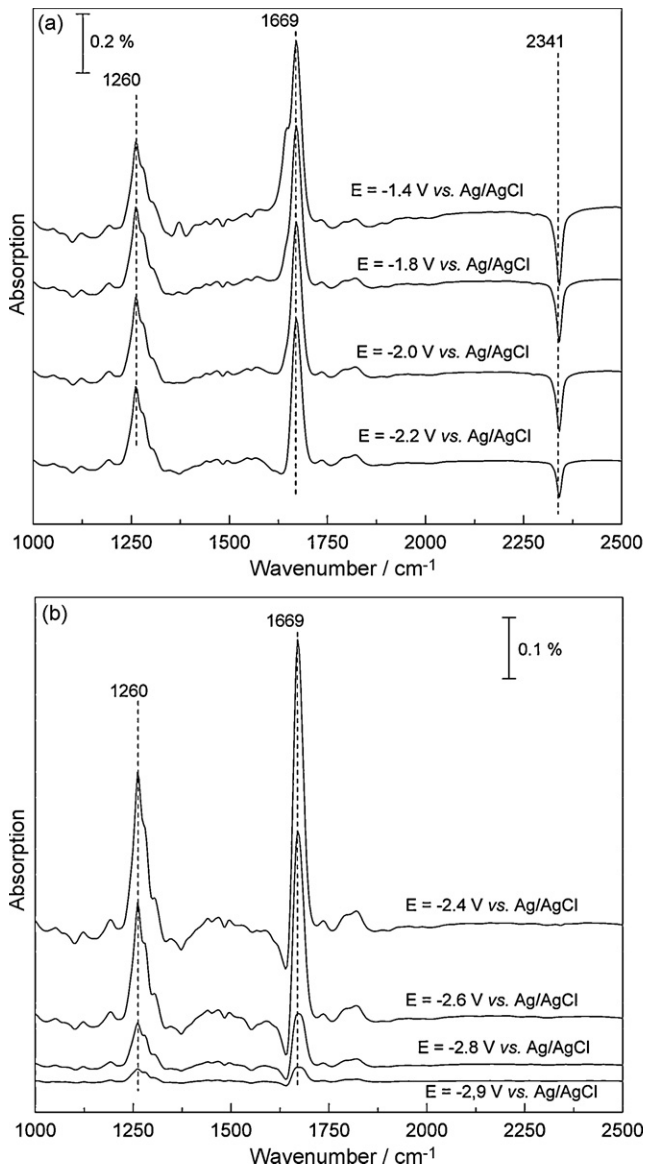

Fig. 6. SPAIR spectra of CO_2-saturated in 0.2 M TEAP–PrC on a Pb electrode at various potentials, R_{Eref} taken at −3.0 V *vs.* Ag/AgCl.

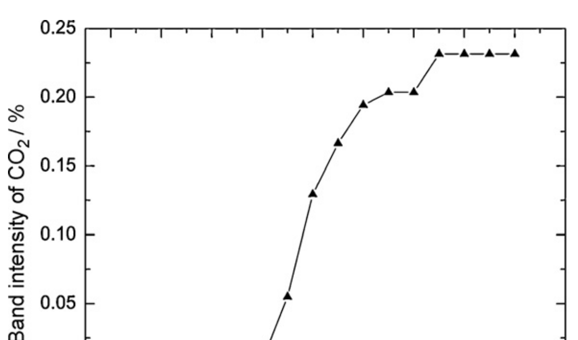

Fig. 7. Evolution of band intensity of CO_2 in 0.2 M TEAP–PrC during a negative going scan of reduction on a Pb electrode. IR band intensities obtained from SPAIR spectra of Fig. 5.

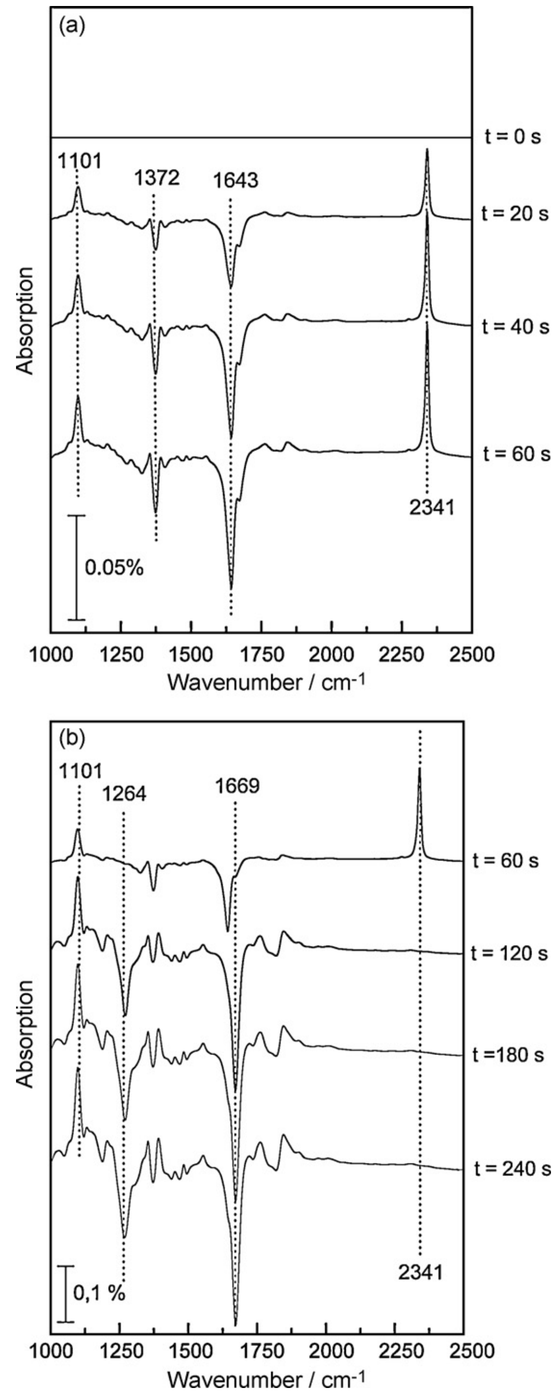

Fig. 8. Spectra of the reduction of CO_2-saturated in 0.2 M TEAP–PrC on a Pb electrode recorded during chronoamperometry measurements at −2.5 V *vs.* Ag/AgCl, R_{ref} taken at t = 0 s.

electrode surface explaining the band intensity becomes almost zero.

3.4. SPAIRS/chronoamperometry

Chronoamperometry/FTIRS measurements were performed at −2.5 V *vs.* Ag/AgCl. The reference spectrum is first taken at t = 0, which means that the positive absorption bands correspond to the consumption of species, while the negative absorption bands can be ascribed to the production of species (Fig. 8). The subtractively normalized infrared spectra show that CO_2 is regularly consumed at the lead electrode. At 120 s the band due to this species

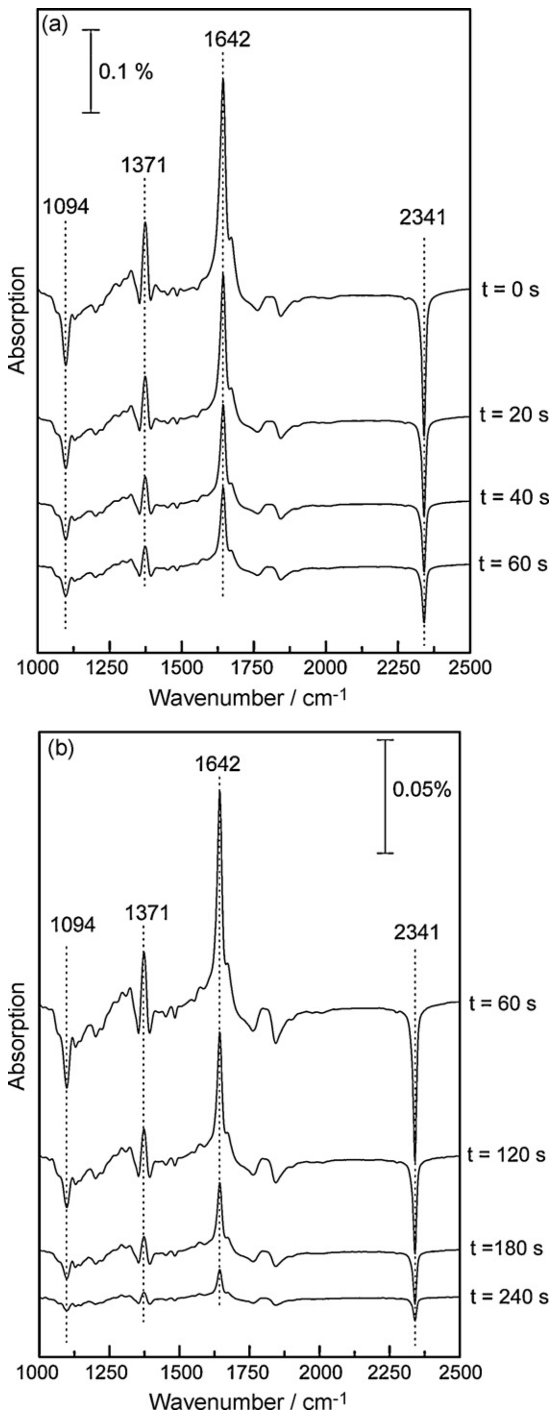

Fig. 9. Spectra of the reduction of CO_2-saturated in 0.2 M TEAP-PrC on a Pb electrode recorded during chronoamperometry measurements at −2.5 V *vs.* Ag/AgCl, R_{ref} taken at t = 300 s.

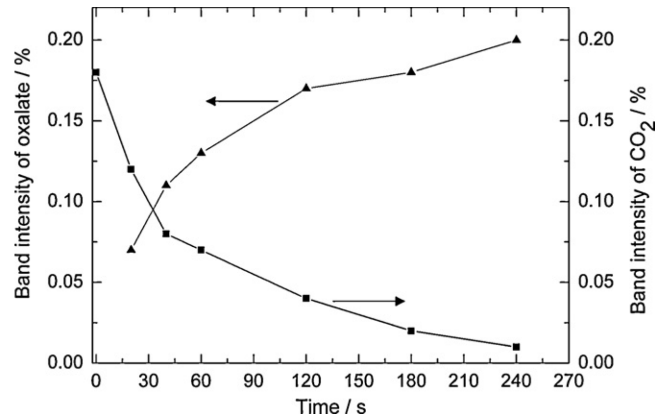

Fig. 10. Evolution of band intensity of CO_2 and oxalate *vs.* time during chronoamperometry measurements at −2.5 V *vs.* Ag/AgCl. IR band intensities obtained from SPAIR spectra of Figs. 7 and 8.

(2341 cm^{-1}) disappears completely. During the same period the band at 1643 cm^{-1} which is characteristic to oxalate appears and increases continuously with time. In addition we observe a band with a constant intensity at 1101 cm^{-1}, which is probably due to the presence of perchlorate ions (ClO_4^-) in the electrolyte [47].

The spectra obtained by SPAIRS/chronoamperometry experiments at −2.5 V *vs.* Ag/AgCl are also recalculated by taking a reference spectrum at t = 300 s. This normalization induces negative absorption bands due to the consumption of species, while the positive absorption bands result in the production of species (Fig. 9). The decrease in the intensity of the band due to CO_2 (2341 cm^{-1}) is concomitant to the increase in that of oxalate centred at 1642 cm^{-1}, as can be observed in Fig. 10.

In Figs. 8 and 9, a band at 1371 is until now not assigned. It is unlikely that this band is due to formate adsorbed at the lead surface, but we tentatively attribute this vibration mode to Pb-CO_2^- species, as suggested by Christensen et al. [48]. This absorption band is intimately linked to that at 1669 cm^{-1}. At the same time they are negative (Fig. 8) and positive (Fig. 9) as reaction products when the reference spectrum is set at t = 0 and t = 300 s, respectively. As pointed out above, the reduction of CO_2 at the Pb electrode surface is very selective since it leads directly to a dimerization product (oxalate) without a side-product such as carbon monoxide. This is may be due to the fact that the instability of the intermediate $CO_2^{\bullet}$ [48] evolves quickly to Pb-CO_2^-.

From the different results, it is possible to infer a reduction mechanism of carbon dioxide on lead electrode in aprotic organic medium. It may be assumed that CO_2 is reduced as follows:

The first step is the adsorption of CO_2, as previously shown by Ikeda et al. [23]:

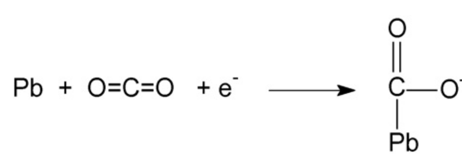

(6)

This feature may be assigned to the absorption band at 1200–1400 cm^{-1}. Then electrodimerization could occur by the interaction between two adsorbed species, which can be observed in the SPAIR spectra with a band centred at 1642 cm^{-1}:

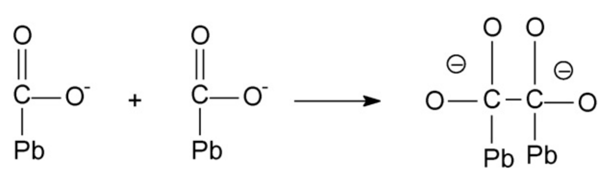

(7)

Finally the desorption of the species could be written:

(8)

This assumption is supported by *in situ* IR spectroscopy measurements close to the electrode surface. For a more complete study of

the reaction mechanism of CO_2 reduction in propylene carbonate, a chromatographic analysis of the bulk electrolytic solution after a long-term electrolysis is in progress.

4. Conclusion

The electroreduction of carbon dioxide was investigated combining a voltammetry study with the *in situ* IR reflectance spectroscopy measurements that allowed a better characterization of the electrochemical behaviour at the surface of a Pb electrode. The experiments performed in propylene carbonate, an aprotic solvent, indicated, without any chemical transformation in the bulk solution, that the CO_2 reduction reaction is a mass transfer process. In spite of difficulties to differentiate the specific bands of the solvent (PrC) and those resulting in the adsorption of carbon dioxide, it was shown by FTIR spectroscopy that the main reaction product is oxalate. The chronoamperometry/FTIRS experiment is a technique well adapted to provide evidence of the consumption of carbon dioxide. When applying an electrode potential of −2.5 V *vs*. Ag/AgCl during 300 s, the decrease in the band intensity due to CO_2 (2341 cm^{-1}) was observed, while that attributable to oxalate appears at 1642 cm^{-1} and increases.

These experiments have demonstrated the absence of a band at 2037 cm^{-1}, which is other evidence that the CO_2 reduction at Pb does not give CO as intermediate or final product under these operating conditions. In addition, this reduction process in a 0.2 M TEAP-PrC solution at the metal surface of the sp group such as Pb leads selectively to the dimerization of CO_2. The adsorbed species determined by *in situ* FTIRS measurements support the proposed mechanism of this reaction in aprotic medium. A chromatographic analysis of the bulk solution after electrolytic experiments will give more detail in the final reaction product. This complementary study is in progress.

Acknowledgement

The authors would like to thank Dr. F. Hahn-Melendres for her help in FTIRS studies.

References

[1] Y. Hori, A. Murata, Electrochim. Acta 35 (1990) 1777–1780.
[2] M. Azuma, K. Hashimoto, M. Hiramoto, M. Watanabe, T. Sakata, J. Electroanal. Chem. 260 (1989) 441–445.
[3] M. Azuma, K. Hashimoto, M. Watanabe, T. Sakata, J. Electroanal. Chem. 294 (1990) 299–303.
[4] M. Watanabe, M. Shibata, A. Katoh, T. Sakata, M. Azuma, J. Electroanal. Chem. 305 (1991) 319–328.
[5] K. Hara, A. Kudo, T. Sakata, J. Electroanal. Chem. 386 (1995) 257–260.
[6] K. Hara, A. Kudo, T. Sakata, J. Electroanal. Chem. 421 (1997) 1–4.
[7] K. Hara, A. Tsuneto, A. Kudo, T. Sakata, J. Electroanal. Chem. 434 (1997) 239–243.
[8] Y. Hori, in: C. Vayenas, et al. (Eds.), Modern Aspects of Electrochemistry, Springer, New York, 2008, pp. 89–189.
[9] R. Ortiz, O.P. Márquez, J. Márquez, C. Gutiérrez, J. Electroanal. Chem. 390 (1995) 99–107.
[10] M. Jitaru, D.A. Lowy, M. Toma, B.C. Toma, L. Oniciu, J. Appl. Electrochem. 27 (1997) 875–889.
[11] R.P.S. Chaplin, A.A. Wragg, J. Appl. Electrochem. 33 (2003) 1107–1123.
[12] K. Subramanian, K. Asokan, D. Jeevarathinam, M. Chandrasekaran, J. Appl. Electrochem. 37 (2007) 255–260.
[13] M. Gattrell, N. Gupta, A. Co, J. Electroanal. Chem. 594 (2006) 1–19.
[14] F. Köleli, T. Röpke, C.H. Hamann, Electrochim. Acta 48 (2003) 1595–1601.
[15] H. Li, C. Oloman, J. Appl. Electrochem. 35 (2005) 955–965.
[16] H. Li, C. Oloman, J. Appl. Electrochem. 36 (2006) 1105–1115.
[17] C. Oloman, H. Li, ChemSusChem 1 (2008) 385–391.
[18] S. Kaneco, K. Iiba, N.-h. Hiei, K. Ohta, T. Mizuno, T. Suzuki, Electrochim. Acta 44 (1999) 4701–4706.
[19] S. Kaneco, N.-h. Hiei, Y. Xing, H. Katsumata, H. Ohnishi, T. Suzuki, K. Ohta, Electrochim. Acta 48 (2002) 51–55.
[20] S. Kaneco, K. Iiba, H. Katsumata, T. Suzuki, K. Ohta, Electrochim. Acta 51 (2006) 4880–4885.
[21] S. Kaneco, K. Iiba, H. Katsumata, T. Suzuki, K. Ohta, J. Solid State Electrochem. 11 (2007) 490–495.
[22] B. Innocent, D. Liaigre, D. Pasquier, F. Ropital, J.M. Léger, K. Kokoh, J. Appl. Electrochem. 39 (2009) 227–232.
[23] S. Ikeda, T. Takagi, K. Ito, Bull. Chem. Soc. Japan 60 (1987) 2517–2522.
[24] K. Ito, S. Ikeda, N. Yamauchi, T. Iida, T. Takagi, Bull. Chem. Soc. Japan 58 (1985) 3027–3028.
[25] Y. Tomita, S. Teruya, O. Koga, Y. Hori, J. Electrochem. Soc 147 (2000) 4164–4167.
[26] Y.B. Vassiliev, V.S. Bagotsky, N.V. Osetrova, O.A. Khazova, N.A. Mayorova, J. Electroanal. Chem. 189 (1985) 271–294.
[27] Y.B. Vassiliev, V.S. Bagotzky, O.A. Khazova, N.A. Mayorova, J. Electroanal. Chem. 189 (1985) 295–309.
[28] Y.B. Vassiliev, V.S. Bagotzky, N.V. Osetrova, A.A. Mikhailova, J. Electroanal. Chem. 189 (1985) 311–324.
[29] I. Taniguchi, B. Aurian-Blajeni, J.O.M. Bockris, Electrochim. Acta 29 (1984) 923–932.
[30] J.O.M. Bockris, J.C. Wass, Mater. Chem. Phys. 22 (1989) 249–280.
[31] M.C. Arévalo, C. Gomis-Bas, F. Hahn, B. Beden, A. Arévalo, A.J. Arvia, Electrochim. Acta 39 (1994) 793–799.
[32] B. Beden, A. Bewick, C. Lamy, J. Electroanal. Chem. 148 (1983) 147–160.
[33] B. Beden, A. Bewick, M. Razaq, J. Weber, J. Electroanal. Chem. 139 (1982) 203–206.
[34] M.L. Marcos, J.G. Velasco, F. Hahn, B. Beden, C. Lamy, A.J. Arvia, J. Electroanal. Chem. 436 (1997) 161–172.
[35] Y. Hori, A. Murata, T. Tsukamoto, H. Wakebe, O. Koga, H. Yamazaki, Electrochim. Acta 39 (1994) 2495–2500.
[36] O. Koga, Y. Hori, Electrochim. Acta 38 (1993) 1391–1394.
[37] Y. Hori, R. Takahashi, Y. Yoshinami, A. Murata, J. Phys. Chem. B 101 (1997) 7075–7081.
[38] K.W. Frese, S. Leach, J. Electrochem. Soc. 132 (1985) 259–260.
[39] B. Innocent, D. Pasquier, F. Ropital, F. Hahn, J.M. Léger, K.B. Kokoh, Appl. Catal. B: Environ. 94 (2010) 219–224.
[40] D.S. Corrigan, M.J. Weaver, J. Electroanal. Chem. 239 (1988) 55–66.
[41] B. Beden, F. Largeaud, K.B. Kokoh, C. Lamy, Electrochim. Acta 41 (1996) 701–709.
[42] A.J. Bard, L.R. Faulkner, Electrochemical Methods, Fundamentals and Applications, Wiley, New York, 1980.
[43] P. Parpot, K.B. Kokoh, B. Beden, C. Lamy, Electrochim. Acta 38 (1993) 1679–1683.
[44] B.R. Eggins, C. Ennis, R. McConnell, M. Spence, J. Appl. Electrochem. 27 (1997) 706–712.
[45] E.M.S. Macoas, R. Fausto, M. Pettersson, L. Khriachtchev, M. Rasanen, J. Phys. Chem. A 104 (2000) 6956–6961.
[46] A. Berná, A. Rodes, J.M. Feliu, Electrochim. Acta 49 (2004) 1257–1269.
[47] P.A. Brooksby, W.R. Fawcett, Spectrochim. Acta Part A: Mol. Biomol. Spectrosc. 64 (2006) 372–382.
[48] P.A. Christensen, A. Hamnett, S.J. Higgins, J.A. Timney, J. Electroanal. Chem. 395 (1995) 195–209.